Numerical investigation of an ammonia-water absorption-compression high-temperature heat pump for hot water and steam production in food processing

Shuai REN*[a], Marcel Ulrich AHRENS [a], Khalid HAMID[a], Ignat TOLSTOREBROV[a], Armin HAFNER[a], Trygve EIKEVIK[a], Kristina N. WIDELL[b]

[a] Norwegian University of Science and Technology, Trondheim, 7194, Norway
[b] SINTEF Ocean, Trondheim, 7465, Norway
* shuai.ren@ntnu.no

ABSTRACT

To achieve climate neutrality in the food sector, there is an urgent need for eco-friendly steam boilers. The absorption-compression heat pumps (ACHP) using an ammonia-water mixture as working fluid can provide a high heat sink temperature at low discharge pressure levels and with temperature glides in absorption and desorption. The present study aims to investigate the performance of the ACHP for hot water and steam production. The simulation model was established based on an ACHP prototype in a NTNU lab. A case of 150 kW heating capacity was simulated with a high pressure of 23.65 bar and a low pressure of 4 bar. The system COP was 2.85 for a pressurized hot water supply temperature of 105 °C. The system performance at different temperature lifts with different heat source inlet temperatures was investigated. In addition, the effects of rich solution composition and compressor intercooling on the system performance were also analyzed.

Keywords: High-temperature Heat Pump, Steam Production, Ammonia-water Mixture, Absorption-compression, Energy Efficiency

1. INTRODUCTION

Process steam and hot water are widely used in food processing for various purposes such as sterilization, drying, cooking, and cleaning. Currently, process steam is mainly produced by fossil fuel boilers, which is nearly one-third of the total energy consumption in the food industry. To achieve climate neutrality in the food sector and reduce greenhouse gas (GHG) emissions, there is an imperative need to phase out fossil fuels by renewable energies or eco-friendly steam generation technologies.

High-temperature heat pumps (HTHPs) were found to be competitive for boiler substitution with high energy efficiencies, low operating costs, and low CO_2 emissions (Bergamini et al., 2019; Bless et al., 2017). Supplying heat with a temperature of more than 100 °C and up to 150 °C is realizable with industrial HTHPs (Arpagaus et al., 2018; Mateu-Royo et al., 2021). The major constraint of utilizing HTHPs is the compressor operating limitations due to the degeneration of lubrication oil at high temperatures (Ommen et al., 2015). Employing liquid-resistant compressors with liquid injection is a potential solution for overcoming this limitation (Zaytsev, 2003).

Absorption-compression heat pumps (ACHP) using zeotropic ammonia-water mixture as the working fluid are an appropriate HTHP solution (Ahrens et al., 2021). The ACHPs can provide high heat sink temperatures up to 140°C at low discharge pressure levels and with temperature glides in absorption and desorption processes. Compared with applying gas boilers, ACHPs are more economical (Jensen et al., 2015). Using an oil-free twin-screw compressor with liquid injection, the compressor discharge temperature can be

decreased (Ahrens et al., 2023), which can ensure the safe operation of the ACHP with a high heat supply temperature.

The present study aims to investigate the performance of the ACHP for hot water and steam production. The simulation model was established based on an ACHP prototype in a NTNU lab in Norway. A case of 150 kW heating capacity was simulated with a high pressure of 23.65 bar and a low pressure of 4 bar. The system performance was investigated at different temperature lifts with different heat source inlet temperatures. The effects of rich solution composition and compressor intercooling on the system performance were also analyzed.

2. METHOD

A numerical model of an ACHP system was developed based on the ACHP prototype in the NTNU lab. The details are described in this section.

2.1. The ACHP process description

A principle sketch of the ACHP system for steam generation is illustrated in Figure 1. The ACHP using ammonia and water mixture as the working fluid was designed based on the Osenbrück cycle (Osenbrück, 1895) as a vapor compression cycle with an additional liquid circuit.
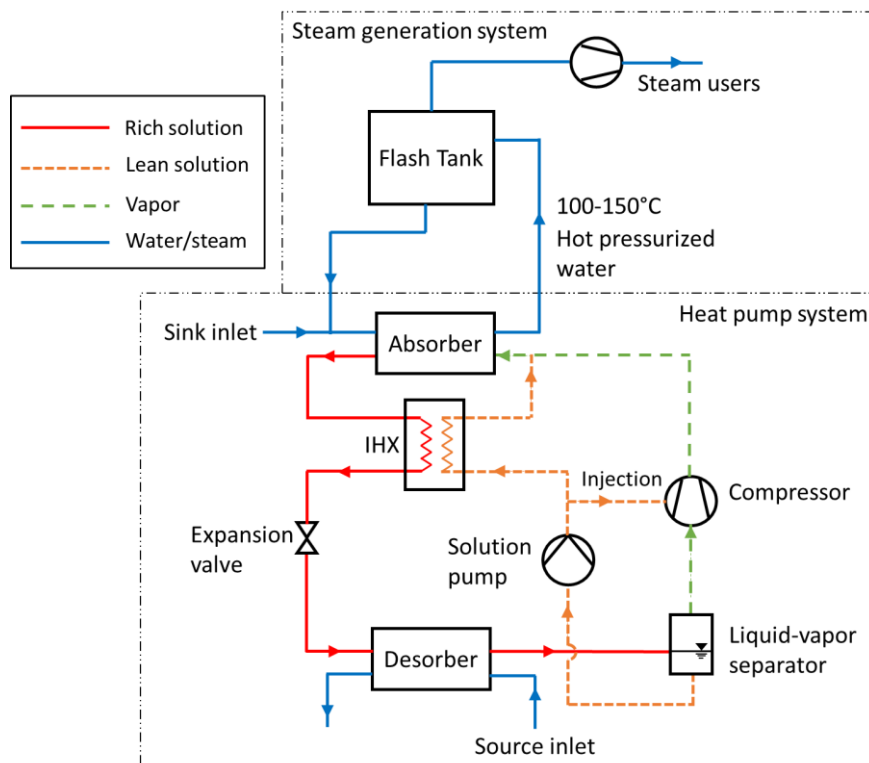
Figure 1: A principle sketch of the ACHP system for steam generation

The cycle consists of a compressor, an absorber, a desorber, an internal heat exchanger (IHX), an expansion valve, a solution pump, and a liquid-vapor separator. Low-grade heat from the heat source is transferred to the refrigerant in the desorber. Vapor containing the predominantly low boiling component of the working fluid mixture is generated in the desorber at a non-constant temperature glide. At the outlet of the desorber, the working fluid is a liquid-vapor two-phase mixture. The liquid phase has a lean concentration of ammonia. The liquid and vapor phases are separated in the liquid-vapor separator to make sure only the vapor enters the compressor. The lean solution from the bottom of the separator is pressurized by the solution pump to the high pressure and then heated by the rich solution in the IHX. The vapor is compressed to the high pressure with a high discharge temperature by the compressor. The compressor is working at the oil-free

condition and the high-pressure lean solution downstream the solution pump is injected into the compressor for lubrication and cooling. The vapor and lean solution are mixed in a mixer before entering the absorber. The ammonia is absorbed into the lean solution inside the absorber and heat is released to the heat sink. The resulting rich ammonia solution leaving the absorber goes into the IHX and is subcooled by the lean solution. Then the rich solution is throttled to the low pressure by the expansion valve resulting in a liquid-vapor mixture which is fed to the desorber.

Pressurized water is used as the heat sink. In the absorber, the temperature of the sink water can be increased to 100-150°C. Then the hot pressurized water is flashed in a flash tank by a throttle valve and supplied to different steam users by a steam compressor. The hot pressurized water can also be directly supplied to hot water users in different food processes.

2.2. Experimental test facility

To investigate the performance of the ACHP steam generation system and each component, an experimental prototype of the ACHP named "Osenbrück 4.0 Heat Pump" was established in a NTNU lab based on the basic ACHP cycle illustrated in Figure 1 but without the steam generation loop, as shown in Figure 2. The system was designed for a maximum heat capacity of 200 kW with a maximum operating pressure of 40 bar and an operational temperature ranging from -10 °C to 190 °C. The test facility consists of an absorption-compression heat pump system and an auxiliary system which provides the required heat source and heat sink water circuits.

Figure 2: The ACHP prototype in the NTNU lab

2.3. Thermodynamic modelling of the ACHP

The performance modelling of the ACHP was conducted by Dymola (Dynamic Modelling Library, version 2022, Dassault systems) (Systèmes, 2022) using Modelica language. Two commercial Modelica libraries were utilized for the simulations, namely TIL-suite 3.10.0 and TILMedia 3.10.0 which are provided by TLK-Thermo GmbH. The ACHP system model and component models were all built based on the "Osenbrück 4.0 Heat Pump" prototype in the NTNU lab. A simplified simulation model of the ACHP is illustrated in Figure 3.

To simplify the simulation, the pressure drops caused by friction in the system and heat losses to the surroundings were neglected. The mixing of the weak solution and vapor at the absorber inlet was assumed

adiabatic. In the liquid-vapor separator, the liquid and vapor phases were assumed at thermodynamic equilibrium.

Figure 3: Simplified Dymola model of the ACHP

The ammonia mass fraction of the rich solution was determined based on the desired temperature levels and glides in the desorber and absorber at certain low pressure and high pressure. The system temperature lift is defined as the temperature difference between the heat sink outlet temperature and the heat source inlet temperature. The circulation ratio (CR) is defined as the mass flow rate ratio between the lean solution and the rich solution. In the present study, the rich solution mass fraction of 0.6 was used for the simulation. The circulation ratio is determined by the vapor quality (q_8) at the outlet of the desorber (CR = 1-q_8). The ammonia mass fraction of the lean solution is also determined by the state at the outlet the desorber because of the thermodynamic equilibrium. The system COP (coefficient of performance) is calculated as:

$$COP = \frac{\dot{Q}_{abs}}{\dot{W}_{com}+\dot{W}_{pump}}$$ Eq. (1)

where $\dot{Q}_{abs}$ is the heat load (kW) in the absorber, $\dot{W}_{com}$ is the shaft power (kW) of the compressor, $\dot{W}_{pump}$ the shaft power (kW) of the solution pump.

2.3.1. Compressor

The compressor of the ACHP prototype is an oil-free twin-screw compressor with liquid injection of the lean solution for lubrication, cooling, and sealing. The compressor has a built-in volume ratio of 3.65. The compression process was simulated by dividing it into two stages with an intercooler to model the liquid injection effect. The intermediate pressure (p_{int}) was determined by the low pressure (p_{LP}, suction pressure) and the high pressure (p_{HP}, discharge pressure) as $p_{int} = \sqrt{p_{LP} \cdot p_{HP}}$. The isentropic efficiency and volumetric efficiency of the compressor used in the simulation were both 0.7. The speed of the low-stage compressor was controlled by the intermediate pressure and the speed of the high-stage compressor was controlled by the desired heat sink outlet temperature by PI controllers. The intercooler was modelled by a tube heat exchanger with a heat boundary which can provide a constant cooling load.

2.3.2. Heat exchangers

All heat exchangers used for the ACHP prototype are plate heat exchangers manufactured by Alfa Laval AS. The plate dimensions of the heat exchangers are listed in Table 1. In all the heat exchangers, the fluids on different sides of the plates flow counter-currently to enhance the heat transfer. Because there is no appropriate correlation for absorption and desorption found in literatures, the heat transfer was calculated by different correlations for approximation, as listed in Table 2. Constant heat transfer coefficients were used in the simulation. The pressure drops inside the heat exchangers were neglected.

Table 1. Plate dimensions of the heat exchangers

	Desorber	Absorber	IHX
Number of plates	40	40	20
Length (m)	0.9	0.9	0.25
Width (m)	0.111	0.111	0.111
Corrugation angle (°)	50	65	65
Wall thickness (m)	0.0004	0.0004	0.0004
Pattern Amplitude (m)	0.002	0.002	0.002
Pattern wave length (m)	0.007	0.007	0.007

Table 2. Heat transfer coefficient correlations applied to the heat exchangers

	Water	Refrigerant
Desorber	Martin (1996)	Taboas et al. (2012) with Martin (1996) for liquid phase heat transfer
Absorber	Martin (1996)	Bell (1972) with Martin (1996) for vapor phase heat transfer and Yan et al. (1999) for liquid phase heat transfer
	Rich solution	Lean solution
IHX	Martin (1996)	Martin (1996)

2.3.3. Separator, solution pump and expansion valve

The liquid-vapor separator prevents the vapor phase entering the compressor and vapor phase entering the solution pump. It also serves as a buffer tank in the ACHP prototype system. The volume of the separator is 196 l. In the simulation, the real volume of the separator was used and the filling level was set at 50%.

In the simulation, the solution pump was operated at a constant mass flow rate which was determined by the circulation ratio. The pump efficiency was assumed to be 0.4. The expansion process was assumed to be isenthalpic and at the outlet of the expansion valve, the liquid-vapor two phase flow was at thermodynamic equilibrium state. The opening area of the expansion valve was adjusted to control the low pressure of the heat pump by a PI controller.

3. RESULTS AND DISCUSSION

To investigate the performance of the ACHP prototype "Osenbrück 4.0 Heat Pump" in NTNU lab for hot water and steam production, a case of 150 kW heating capacity was simulated. The operating parameters are listed in Table 3. The heat sink fluid is pressurized water which can be used as supply water for the steam generation system, as shown in Figure 1.

Table 3. Operating parameters applied to the simulation

Source inlet temperature	70 °C
Sink inlet temperature	75 °C
Low pressure	4 bar
High pressure	23.65 bar
Intermediate pressure	9.7 bar
Rich solution mass fraction	0.6
Circulation ratio	0.59

3.1. System performance

The simulation results are illustrated in Table 4. The state point number of streams is according to Figure 3. The pressure in the desorber was controlled by adjusting the opening of the expansion valve and was maintained at 4 bar. The vapor quality at the outlet of the desorber is 0.41 and the circulation ratio is 0.59. At the high pressure of 23.65 bar, the obtained sink outlet temperature is 105 °C and the COP of the ACHP system is 2.85. The compressor intercooling load was determined by injecting the high-pressure lean solution (stream no.10, downstream the solution pump and upstream the IHX) with 15 % of the compressor's suction mass flow rate. With the intercooling, the compressor discharge temperature was decreased from 276 °C to 160.3 °C.

Table 4. Simulation results of the ACHP system

ith stream	Mass flow rate (kg/s)	Ammonia mass fraction (-)	Temperature (°C)	Pressure (bar)
1	0.1183	0.975	57.7	4
2	0.1183	0.975	157.3	9.7
3	0.1183	0.975	160.3	23.65
4	0.2887	0.6	118.5	23.65
5	0.2887	0.6	88.5	23.65
6	0.2887	0.6	84	23.65
7	0.2887	0.6	30	4
8	0.2887	0.6	57.7	4
9	0.1703	0.35	57.7	4
10	0.1703	0.35	61.1	23.65
11	0.1703	0.35	81.2	23.65
12	0.1183	0.975	72.7	9.7
13	1.2	-	70	5
14	1.2	-	44.95	5
15	1.2	-	75	10
16	1.2	-	105	10

3.2. Effects of temperature lift on the system performance

The COPs and rich solution mass flow rates at different temperature lifts with different heat source inlet temperatures are illustrated in Figure 4. The rich solution ammonia mass fraction was maintained at 0.6 and the low pressure was kept at 4 bar for all the simulated conditions. In addition, the source and sink fluid mass flow rates and sink fluid inlet temperature were maintained at constant values as shown in Table 4.

It is obvious that with the increase of the temperature lift the system COP is decreased and the required rich solution mass flow rate is increased. This is because at a certain source fluid inlet temperature, the heat capacity of the heat pump is increased with the increase of the temperature lift. More heat is required to be

provided by the vapor compression and higher refrigerant mass flow rates are needed for the heat transportation. In addition, at the same temperature lift, higher system COPs were observed at lower source inlet temperatures. This is because the heat load to the sink side is lower with lower sink outlet temperatures. Therefore, the required pressure in the absorber is lower which results in lower power consumption of the compressor and better system performance. Furthermore, as shown in Figure 4, the required rich solution mass flow rate mainly depends on the sink outlet temperature which decides the heating load of the ACHP. Similar values are observed for the same sink outlet temperature.
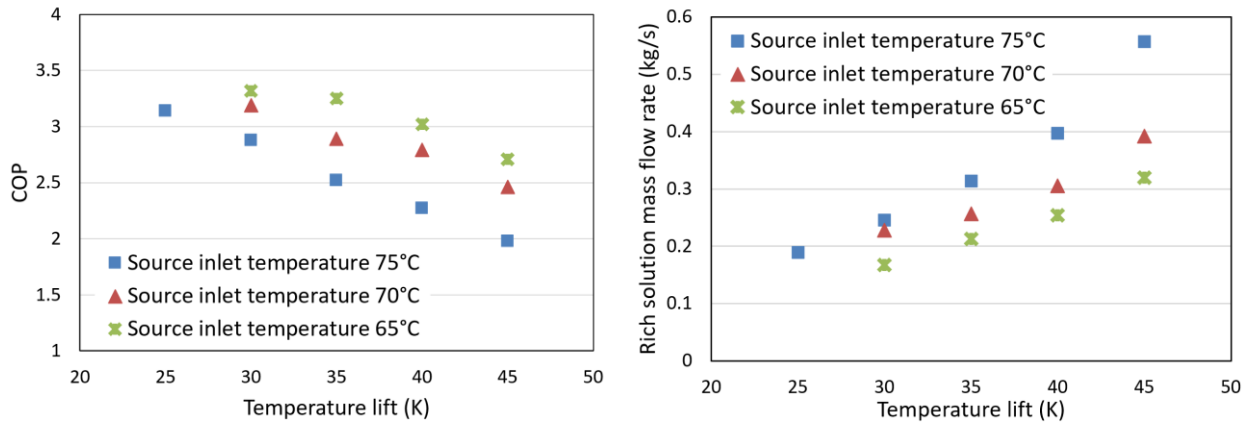
Figure 4: COPs and rich solution mass flow rates at different temperature lifts
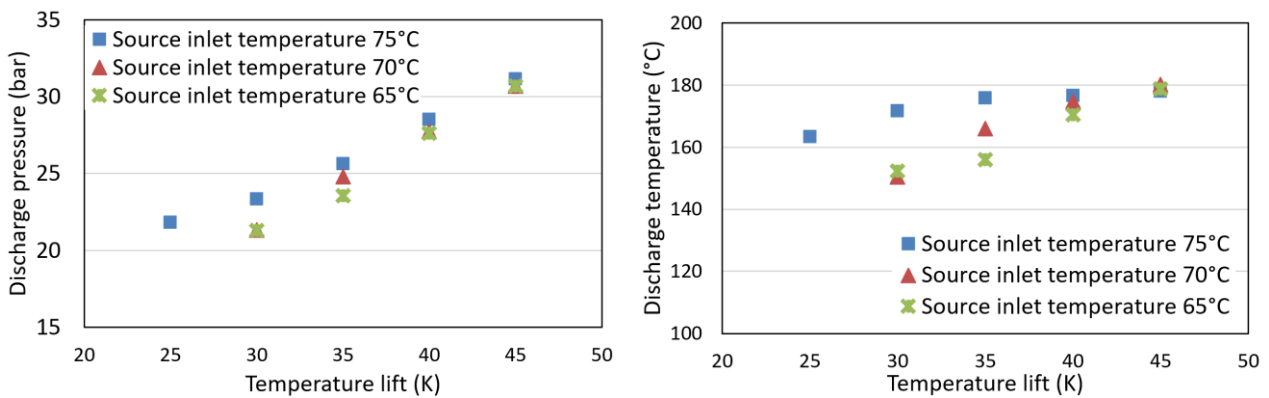
Figure 5: Discharge pressures and temperatures at different temperature lifts
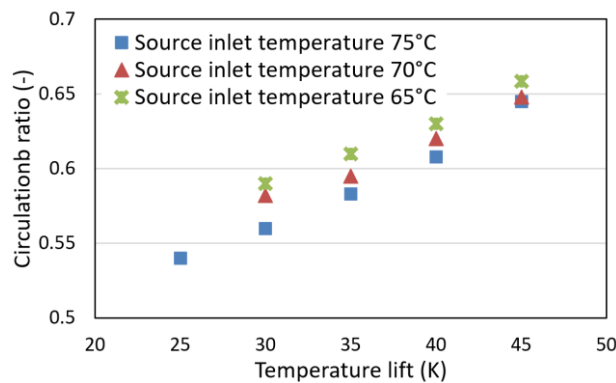
Figure 6: Circulation ratios at different temperature lifts

The compressor discharge pressures and temperatures at different temperature lifts are illustrated in Figure 5. With the increase of the temperature lift, the heat load to the heat sink side is increased so that the required pressure in the absorber and the consequent compressor discharge temperature are also increased. Moreover, at the same temperature lift, higher sink outlet temperatures require higher pressures in the

absorber so that the discharge pressures and temperatures are higher for the cases with higher source inlet temperatures. However, the difference between the discharge pressures at higher and lower sink outlet temperatures is diminishing with the increase of the temperature lift. This is because at higher temperature lifts, the cases with lower source inlet temperatures have much lower rich solution mass flow rates as shown in Figure 4, but higher circulation ratios, as shown in Figure 6, which results in lower suction vapor mass flow rates and lower refrigerant heat flow rate at the inlet of the absorber. Therefore, to achieve the same sink outlet temperature, a much higher pressure is required in the absorber for the cases with lower source inlet temperatures. That is why with the increase of the temperature lift, the discharge pressure increases much faster for the cases with lower source inlet temperatures.

3.3. Effects of rich solution ammonia mass fraction

To investigate the effects of the refrigerant composition on the system performance, three ACHP cycles were simulated with different rich solution ammonia mass fractions of 0.6, 0.65, and 0.7 respectively. The same source inlet temperature of 70 °C, sink inlet temperature of 75 °C and sink outlet temperature of 110 °C were used for the three cycles. The low pressure was maintained at 4 bar. As shown in Figure 7(a), with the increase of the rich solution ammonia mass fraction, the circulation ratio is decreased, which results in the increase of the vapor mass flow rate and the decrease of the lean solution mass flow rate. The increased vapor mass flow rate causes more compressor power consumption and the decrease of the system COP. In addition, because in the simulations, the compressor intercooling load is increased with the increase of the suction vapor mass flow rate, the vapor enthalpy at the compressor discharge is reduced by the increased intercooling load. To obtain the same sink outlet temperature, a higher pressure is required in the absorber for the case with higher rich solution ammonia mass fraction and the consequent discharge temperature is higher, as shown in Figure 7(b).

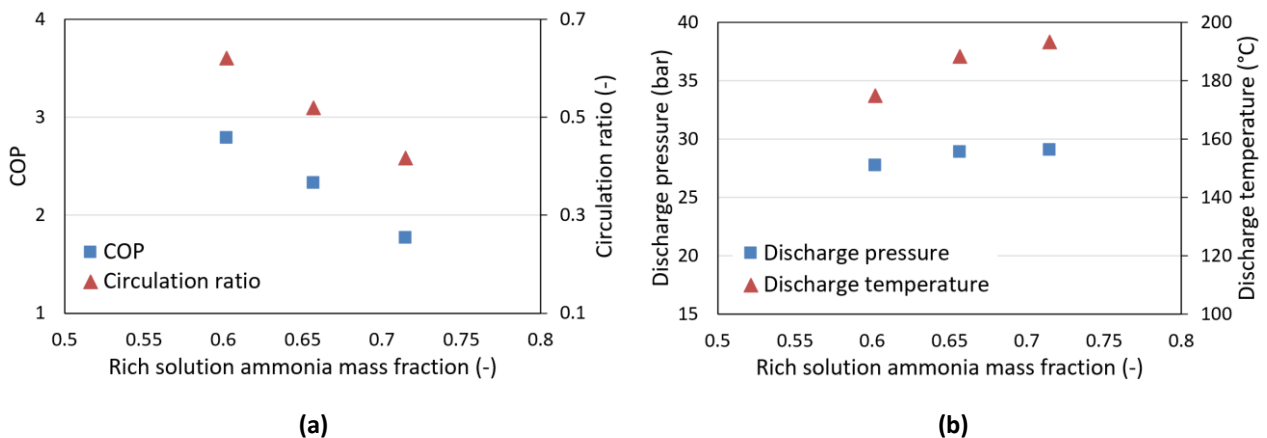(a)   (b)

Figure 7: (a) COPs and circulation ratios at different rich solution ammonia mass fractions (b) discharge pressures at different rich solution ammonia mass fractions

3.4. Effects of compressor intercooling

As discussed above, the compressor intercooling can decrease the compressor discharge temperature and influence the performance of the heat pump. To investigate the effects of the compressor intercooling on the ACHP performance, the case of 150 kW capacity was simulated with different compressor intercooling loads. The operating parameters are as listed in Table 3. As shown in Figure 8(a), by increasing the compressor intercooling load from the injection of the high pressure lean solution with 0 % of the vapor mass flow rate to 25 % of the vapor mass flow rate, the COP of the ACHP is decreased. This is because the removed heat from the vapor compression by the intercooling is compensated by the increase of the vapor mass flow rate. The increased vapor mass flow rate results in the increase of the total refrigerant mass flow rate which causes the increase of the circulation ratio. The increased circulation ratio will again result in the further increase of the total solution mass flow rate. As shown in Figure 8(b), with the increase of the intercooling load, the compressor discharge temperature is decreased and rich solution mass flow rate is increased. The increased

vapor and rich solution mass flow rates will cause the increase of the shaft power of both compressor and solution pump so that the system COP is decreased.

However, this simulation results can only represent the cases of two-stage compression with intercooling. The situation of single stage compression with liquid injection is different because with the injection of lean solution no heat is removed from the heat pump system. There is no need to increase the suction vapor mass flow to compensate the heat loss from compressor intercooling so that the system performance will not be deteriorated. More information about the liquid injection of the compressor can be found in Ahrens et al. (2023).

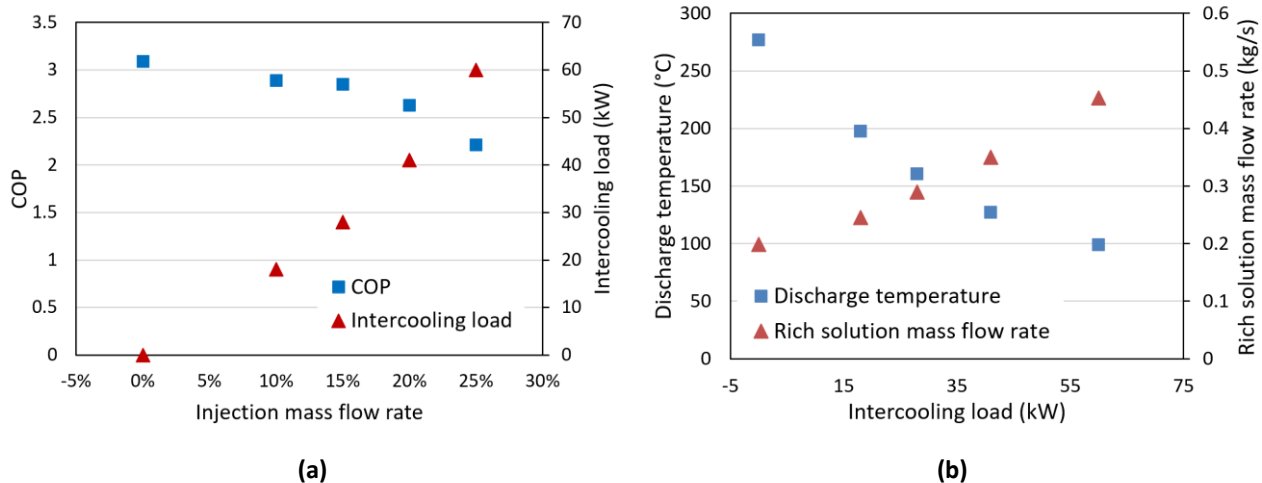(a)   (b)

Figure 8: (a) COPs and compressor intercooling loads at different liquid injection mass flow rates (b) Discharge temperatures and rich solution mass flow rates at different liquid injection mass flow rates

4. CONCLUSIONS

In the present study, the performance of the ACHP using ammonia-water mixture as working fluid for hot water and steam production was investigated numerically. The simulation model was established based on the ACHP prototype "Osenbrück 4.0 Heat Pump" in the NTNU lab. A case of 150 kW heating capacity was simulated with a high pressure of 23.65 bar and low pressure of 4 bar. The ACHP system COP was 2.85 for a pressurized hot water supply temperature of 105 °C. With the increase of the temperature lift, the COP of the ACHP is decreased and the required refrigerant mass flow rate is increased. At the same temperature lift, higher system COPs were observed at lower source inlet temperatures with lower discharge pressures and lower discharge temperatures. In addition, with the increase of the rich solution ammonia mass fraction, the COP is decreased and the discharge pressure is slightly increased. Furthermore, the increase of the compressor intercooling load can decrease the compressor discharge temperature and also decrease the COP of the ACHP. To further investigate the characteristics and performance of the ACHP, the influences of pressure drops should be considered and variable heat transfer coefficients should be used for the heat exchangers. Experimental studies should be conducted to validate the simulation results.

ACKNOWLEDGEMENTS

DATA AVAILABLE STATEMENT

The data supporting reported results can be found in a public repository under the following DIO: https://doi.org/10.18710/EDO53E.

REFERENCES

Ahrens, M. U., Loth, M., Tolstorebrov, I., Hafner, A., Kabelac, S., Wang, R., & Eikevik, T. M. (2021). Identification of Existing Challenges and Future Trends for the Utilization of Ammonia-Water Absorption–Compression Heat Pumps at High Temperature Operation. *Applied Sciences*, *11*(10), 4635.

Ahrens, M. U., Tolstorebrov, I., Tønsberg, E. K., Hafner, A., Wang, R., & Eikevik, T. M. (2023). Numerical investigation of an oil-free liquid-injected screw compressor with ammonia-water as refrigerant for high temperature heat pump applications. *Applied Thermal Engineering*, *219*, 119425.

Arpagaus, C., Bless, F., Uhlmann, M., Schiffmann, J., & Bertsch, S. S. (2018). High temperature heat pumps: Market overview, state of the art, research status, refrigerants, and application potentials. *Energy*, *152*, 985-1010.

Bell, K. J., Ghaly. M.A. (1972). An approximate generalized design method for multicomponent/partial condensers. AIChE Symp. Ser.,

Bergamini, R., Jensen, J. K., & Elmegaard, B. (2019). Thermodynamic competitiveness of high temperature vapor compression heat pumps for boiler substitution. *Energy*, *182*, 110-121.

Bless, F., Arpagaus, C., Bertsch, S. S., & Schiffmann, J. (2017). Theoretical analysis of steam generation methods-Energy, CO2 emission, and cost analysis. *Energy*, *129*, 114-121.

Jensen, J. K., Ommen, T., Markussen, W. B., Reinholdt, L., & Elmegaard, B. (2015). Technical and economic working domains of industrial heat pumps: Part 2–Ammonia-water hybrid absorption-compression heat pumps. *International Journal of Refrigeration*, *55*, 183-200.

Martin, H. (1996). A theoretical approach to predict the performance of chevron-type plate heat exchangers. *Chemical Engineering and Processing: Process Intensification*, *35*(4), 301-310.

Mateu-Royo, C., Arpagaus, C., Mota-Babiloni, A., Navarro-Esbrí, J., & Bertsch, S. S. (2021). Advanced high temperature heat pump configurations using low GWP refrigerants for industrial waste heat recovery: A comprehensive study. *Energy Conversion and Management*, *229*, 113752.

Ommen, T., Jensen, J. K., Markussen, W. B., Reinholdt, L., & Elmegaard, B. (2015). Technical and economic working domains of industrial heat pumps: Part 1–Single stage vapour compression heat pumps. *International Journal of Refrigeration*, *55*, 168-182.

Osenbrück, A. (1895). Verfahren zur kälteerzeugung bei absorptionsmaschinen. *Deutsches Patent*, *84084*.

Systèmes, D. (2022). DYMOLA Systems Engineering: Multi-Engineering Modeling and Simulation based on Modelica and FMI. *En ligne]. Disponible sur: https://www.3ds.com/productsservices/catia/products/dymola/.[Visité le 12 04 2021]*.

Taboas, F., Valles, M., Bourouis, M., & Coronas, A. (2012). Assessment of boiling heat transfer and pressure drop correlations of ammonia/water mixture in a plate heat exchanger. *International Journal of Refrigeration*, *35*(3), 633-644.

Yan, Y.-Y., Lio, H.-C., & Lin, T.-F. (1999). Condensation heat transfer and pressure drop of refrigerant R-134a in a plate heat exchanger. *International Journal of Heat and Mass Transfer*, *42*(6), 993-1006.

Zaytsev, D. V. (2003). Development of wet compressor for application in compression-resorption heat pumps.